SMEFT projections using EIC PVDIS asymmetries

Kağan Şimşek

Northwestern University

in collaboration with

Radja Boughezal, Alexander Emmert, Tyler Kutz, Sonny Mantry,
Michael Nycz, Frank Petriello, Daniel Wiegand, and Xiaochao Zheng

reference: arXiv:2204.07557

INT Workshop: Parity-Violation and other Electroweak Physics
at JLab 12 GeV and Beyond

June 27 – July 1, 2022

- We study NC DIS cross-section asymmetries at EIC.
- We adopt SMEFT framework to parameterize BSM effects.
- Higher-dimensional operators are built of existing SM particles:

$$\mathscr{L}_{\text{SMEFT}} = \mathscr{L}_{\text{SM}} + \sum_{n>4} \frac{1}{\Lambda^{n-4}} \sum_k C_k^{(n)} O_k^{(n)}$$

- All new physics is assumed to be heavier than SM states and accessible collider energy.
- We focus on $n = 6$ and semi-leptonic 4-fermion $O_k^{(n)}$.
- We find that the EIC can
  - probe complementarily and competitively to LHC DY
  - resolve degeneracies observed in LHC NC DY data fits

We study the NC DIS in the process $\ell + H \to \ell' + X$, where $\ell = e^-, e^+$ and $H = p, D$:

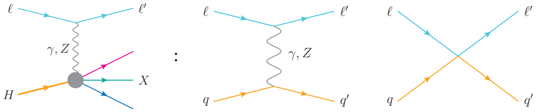

to leading order at parton level

We parameterize the vertex factors in terms of vector and axial couplings:

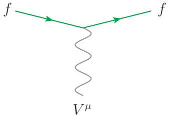

$$i\gamma_\mu g_1^{(fV)} + i\gamma_\mu\gamma_5 g_5^{(fV)},$$

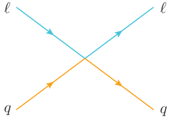

$$\begin{aligned} & i[\gamma_\mu][\gamma^\mu]g_{11}^{(\ell q)} \\ & +i[\gamma_\mu][\gamma^\mu\gamma_5]g_{15}^{(\ell q)} \\ & +i[\gamma_\mu\gamma_5][\gamma^\mu]g_{51}^{(\ell q)} \\ & +i[\gamma_\mu\gamma_5][\gamma^\mu\gamma_5]g_{55}^{(\ell q)} \end{aligned}$$

We don't consider Yukawa or dipole interactions because they are suppressed by fermion masses, which we assume to vanish.

SMEFT operators shift the usual vector and axial SM couplings in a gauge-invariant way: e.g.

$$g_1^{(fZ)} = g_V^f + \mathcal{O}(C_k), \quad g_5^{(fZ)} = g_A^f + \mathcal{O}(C_k)$$

Operators that contribute to the ffV and $\ell\ell qq$ vertices at dimension 6 are (Grzadkowski *et al.* [1008.4884]):

ffV	$\ell\ell qq$
$O_{\varphi\ell}^{(1)} = (\varphi^\dagger i \overleftrightarrow{D}_\mu \varphi)(\bar{\ell}\gamma^\mu \ell)$	$O_{\ell q}^{(1)} = (\bar{\ell}\gamma_\mu \ell)(\bar{q}\gamma^\mu q)$
$O_{\varphi\ell}^{(3)} = (\varphi^\dagger i \overleftrightarrow{D}_\mu \tau^I \varphi)(\bar{\ell}\gamma^\mu \tau^I \ell)$	$O_{\ell q}^{(3)} = (\bar{\ell}\gamma_\mu \tau^I \ell)(\bar{q}\gamma^\mu \tau^I q)$
$O_{\varphi e} = (\varphi^\dagger i \overleftrightarrow{D}_\mu \varphi)(\bar{e}\gamma^\mu e)$	$O_{eu} = (\bar{e}\gamma_\mu e)(\bar{u}\gamma^\mu u)$
$O_{\varphi q}^{(1)} = (\varphi^\dagger i \overleftrightarrow{D}_\mu \varphi)(\bar{q}\gamma^\mu q)$	$O_{ed} = (\bar{e}\gamma_\mu e)(\bar{d}\gamma^\mu d)$
$O_{\varphi q}^{(3)} = (\varphi^\dagger i \overleftrightarrow{D}_\mu \tau^I \varphi)(\bar{q}\gamma^\mu \tau^I q)$	$O_{\ell u} = (\bar{\ell}\gamma_\mu \ell)(\bar{u}\gamma^\mu u)$
$O_{\varphi u} = (\varphi^\dagger i \overleftrightarrow{D}_\mu \varphi)(\bar{u}\gamma^\mu u)$	$O_{\ell d} = (\bar{\ell}\gamma_\mu \ell)(\bar{d}\gamma^\mu d)$
$O_{\varphi d} = (\varphi^\dagger i \overleftrightarrow{D}_\mu \varphi)(\bar{d}\gamma^\mu d)$	$O_{qe} = (\bar{q}\gamma_\mu q)(\bar{e}\gamma^\mu e)$

There is one more:

$O_{\varphi WB} = (\varphi^\dagger \tau^I \varphi) W^I_{\mu\nu} B^{\mu\nu}$ $\Rightarrow$ causes kinetic mixing of W^3 and B

$\Rightarrow$ universally shifts the ffV vertices after diagonalization that gives physical photon and Z boson states

The *ffV* operators are already strongly bounded by Z and W pole observables (Dawson & Giardino [1909.02000]):

ffV	C_k	95% CL, $\Lambda = 1$ TeV
$O_{\varphi\ell}^{(1)} = (\varphi^\dagger i \overleftrightarrow{D}_\mu \varphi)(\bar{\ell}\gamma^\mu \ell)$	$C_{\varphi\ell}^{(1)}$	$[-0.043, 0.012]$
$O_{\varphi\ell}^{(3)} = (\varphi^\dagger i \overleftrightarrow{D}_\mu \tau^I \varphi)(\bar{\ell}\gamma^\mu \tau^I \ell)$	$C_{\varphi\ell}^{(3)}$	$[-0.012, 0.0029]$
$O_{\varphi e} = (\varphi^\dagger i \overleftrightarrow{D}_\mu \varphi)(\bar{e}\gamma^\mu e)$	$C_{\varphi e}$	$[-0.013, 0.0094]$
$O_{\varphi q}^{(1)} = (\varphi^\dagger i \overleftrightarrow{D}_\mu \varphi)(\bar{q}\gamma^\mu q)$	$C_{\varphi q}^{(1)}$	$[-0.027, 0.043]$
$O_{\varphi q}^{(3)} = (\varphi^\dagger i \overleftrightarrow{D}_\mu \tau^I \varphi)(\bar{q}\gamma^\mu \tau^I q)$	$C_{\varphi q}^{(3)}$	$[-0.011, 0.014]$
$O_{\varphi u} = (\varphi^\dagger i \overleftrightarrow{D}_\mu \varphi)(\bar{u}\gamma^\mu u)$	$C_{\varphi u}$	$[-0.072, 0.091]$
$O_{\varphi d} = (\varphi^\dagger i \overleftrightarrow{D}_\mu \varphi)(\bar{d}\gamma^\mu d)$	$C_{\varphi d}$	$[-0.16, 0.060]$
$O_{\varphi WB} = (\varphi^\dagger \tau^I \varphi) W^I_{\mu\nu} B^{\mu\nu}$	$C_{\varphi WB}$	$[-0.0088, 0.0013]$

Thus, we restrict our attention only to the operators contributing to the $\ell\ell qq$ vertex, which leaves us with seven Wilson coefficients of interest: C_{eu}, C_{ed}, $C_{\ell q}^{(1)}$, $C_{\ell q}^{(3)}$, $C_{\ell u}$, $C_{\ell d}$, and C_{qe}.

Since we consider contributions only to the $\ell\ell qq$ interaction, we assume the usual SM ffV vertices in our analysis:

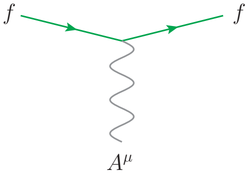

$$g_1^{(fA)} = -eQ_f$$
$$g_5^{(fA)} = 0$$

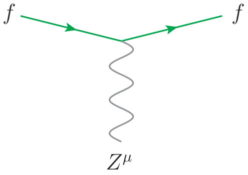

$$g_1^{(fZ)} = g_V^f$$
$$g_5^{(fZ)} = g_A^f$$

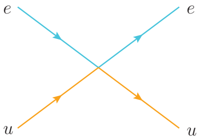

$$\begin{aligned}
g_{11}^{(eu)} &= \tfrac{1}{4}\left[C_{eu} + \left(C_{\ell q}^{(1)} - C_{\ell q}^{(3)}\right) + C_{\ell u} + C_{qe}\right]\\
g_{15}^{(eu)} &= \tfrac{1}{4}\left[C_{eu} - \left(C_{\ell q}^{(1)} - C_{\ell q}^{(3)}\right) + C_{\ell u} - C_{qe}\right]\\
g_{51}^{(eu)} &= \tfrac{1}{4}\left[C_{eu} - \left(C_{\ell q}^{(1)} - C_{\ell q}^{(3)}\right) - C_{\ell u} + C_{qe}\right]\\
g_{55}^{(eu)} &= \tfrac{1}{4}\left[C_{eu} + \left(C_{\ell q}^{(1)} - C_{\ell q}^{(3)}\right) - C_{\ell u} - C_{qe}\right]
\end{aligned}$$

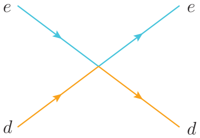

the same as for *eeuu* but with $u \to d$ and $C_{\ell q}^{(1)} - C_{\ell q}^{(3)} \to C_{\ell q}^{(1)} + C_{\ell q}^{(3)}$

Amplitude and cross section for $\ell + q \to \ell' + q'$:

$$\mathscr{M} = \mathscr{M}_\gamma + \mathscr{M}_Z + \mathscr{M}_\times \Rightarrow \mathrm{d}\sigma^{\lambda_\ell \lambda_q} = \frac{\mathrm{d}^2\sigma}{\mathrm{d}x\,\mathrm{d}Q^2} = \frac{1}{16\pi x^2 s^2}\,|\mathscr{M}|^2 + \mathscr{O}(C_k^2)$$

Asymmetry definitions:

- unpolarized PV asymmetries: $A_{\mathrm{PV}} = \dfrac{\mathrm{d}\sigma_\ell}{\mathrm{d}\sigma_0}$
- polarized PV asymmetries: $\Delta A_{\mathrm{PV}} = \dfrac{\mathrm{d}\sigma_H}{\mathrm{d}\sigma_0}$
- lepton-charge asymmetries: $A_{\mathrm{LC}} = \dfrac{\mathrm{d}\sigma_0(e^+H) - \mathrm{d}\sigma_0(e^-H)}{\mathrm{d}\sigma_0(e^+H) + \mathrm{d}\sigma_0(e^-H)}$

where

$$\mathrm{d}\sigma_0 = \frac{1}{4}\sum_q f_{q/H}[\mathrm{d}\sigma^{++} + \mathrm{d}\sigma^{+-} + \mathrm{d}\sigma^{-+} + \mathrm{d}\sigma^{--}] : \text{unpol. } \ell + \text{unpol. } H$$

$$\mathrm{d}\sigma_\ell = \frac{1}{4}\sum_q f_{q/H}[\mathrm{d}\sigma^{++} + \mathrm{d}\sigma^{+-} - \mathrm{d}\sigma^{-+} - \mathrm{d}\sigma^{--}] : \text{pol. } \ell + \text{unpol. } H$$

$$\mathrm{d}\sigma_H = \frac{1}{4}\sum_q \Delta f_{q/H}[\mathrm{d}\sigma^{++} - \mathrm{d}\sigma^{+-} + \mathrm{d}\sigma^{-+} - \mathrm{d}\sigma^{--}] : \text{unpol. } \ell + \text{pol. } H$$

Data sets, shown with beam energies and nominal annual luminosities:

D1	5 GeV $\times$ 41 GeV eD, 4.4 fb^{-1}
D2	5 GeV $\times$ 100 GeV eD, 36.8 fb^{-1}
D3	10 GeV $\times$ 100 GeV eD, 44.8 fb^{-1}
D4	10 GeV $\times$ 137 GeV eD, 100 fb^{-1}
D5	18 GeV $\times$ 137 GeV eD, 15.4 fb^{-1}
P1	5 GeV $\times$ 41 GeV ep, 4.4 fb^{-1}
P2	5 GeV $\times$ 100 GeV ep, 36.8 fb^{-1}
P3	10 GeV $\times$ 100 GeV ep, 44.8 fb^{-1}
P4	10 GeV $\times$ 275 GeV ep, 100 fb^{-1}
P5	18 GeV $\times$ 275 GeV ep, 15.4 fb^{-1}
P6	18 GeV $\times$ 275 GeV ep, 100 fb^{-1}

P6: Yellow Report reference setting [2103.05419]

Data set labels:
D, P: unpolarized PV asymmetry
ΔD, ΔP: polarized PV asymmetry
LD, LP: lepton-charge asymmetry

Cuts on projected data:

$Q > 1$ GeV	to avoid nonperturbative QCD
$y > 0.1$	to avoid bin migration and unfolding uncertainty
$y < 0.9$	to avoid high photoproduction background due to final-state hadron
$\lvert\eta\rvert < 3.5$	to restrict events in main acceptance of ECCE detector
$E' > 2$ GeV	to have high-purity e^- samples

Additional cuts in SMEFT analysis:

$x < 0.5$
$Q > 10$ GeV

to avoid *large* uncertainties from nonperturbative QCD and nuclear dynamics

Phase space of the data sets ($\sqrt{s} = 70$-140 GeV, $0.1 \leq y \leq 0.9$):

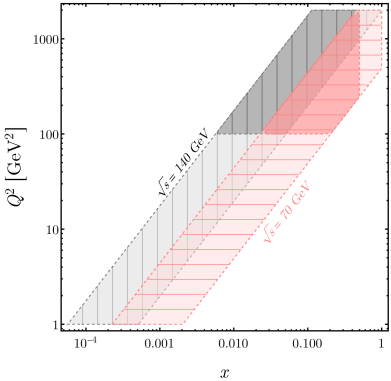

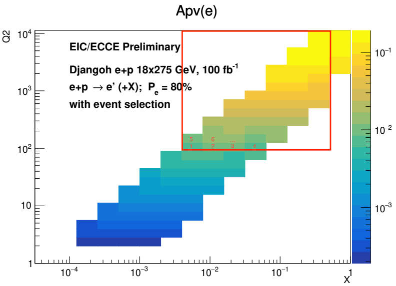

The red box indicates the *good* bins used in our SMEFT analysis.

Error type	A_{PV} (D, P)	ΔA_{PV} (ΔD, ΔP)	A_{LC} (LD, LP)
statistical (NL)	$\sigma_{\mathrm{stat}} = \frac{1}{P_\ell \sqrt{N}}$	$\frac{P_\ell}{P_H}\sigma_{\mathrm{stat}}$	$\sqrt{10}P_\ell\sigma_{\mathrm{stat}}$
statistical (HL)	$\frac{1}{\sqrt{10}}\sigma_{\mathrm{stat}}$	$\frac{1}{\sqrt{10}}\frac{P_\ell}{P_H}\sigma_{\mathrm{stat}}$	✗
uncorrelated systematic	1% rel.	1% rel.	1% rel.
fully correlated beam polarization	1% rel.	2% rel.	✗
fully correlated luminosity	✗	✗	2% abs.
uncorrelated QED NLO	✗	✗	$5\% \times (A_{\mathrm{LC}}^{\mathrm{NLO}} - A_{\mathrm{LC}}^{\mathrm{Born}})$
fully correlated PDF	✓	✓	✓

PDF sets used: `NNPDF3.1 NLO` and `NNPDFpol1.1`

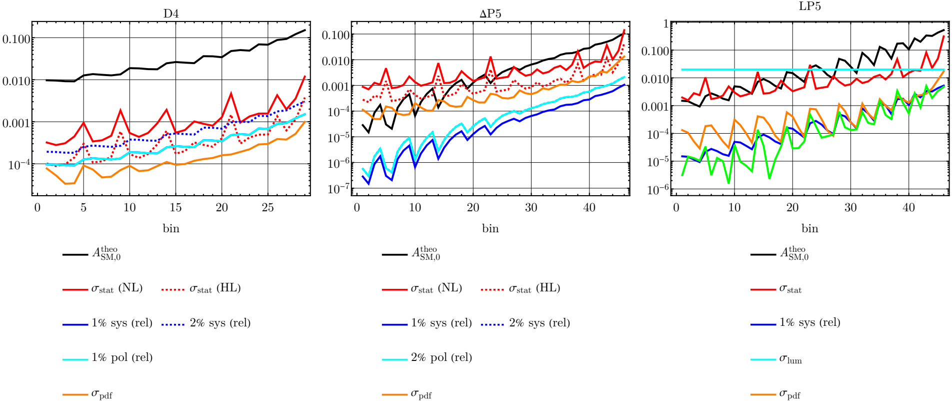

- Bins on the horizontal axes are the *good* x and Q^2 bins.
- Stat error dominates in PV asymmetries in NL case.
- Systematic and beam-polarization errors become comparable to stat error in HL case.
- Luminosity error dominates in LC asymmetries.
- Stat error competes with luminosity error at high-x high-Q^2 bins.
- PDF errors are the least dominant in unpolarized PV asymmetries but become significant in the polarized case.

Pseudodata generation:

$$A^{(e)}_{\text{pseudo},b} = A_{\text{SM},b} + r^{(e)}_b \sigma^{\text{unc}}_b + r'^{(e)} \sigma^{\text{cor}}_b$$

$$b \in \text{Range}(N_{\text{bin}}), \quad e \in \text{Range}(N_{\text{exp}}), \quad N_{\text{exp}} = 10^3, \quad r^{(e)}_b, r'^{(e)} \sim \mathcal{N}(0,1)$$

$$\sigma^{\text{unc}}_b = \sigma_{\text{stat},b} \oplus \sigma_{\text{sys},b} \qquad \sigma^{\text{unc}}_b = \sigma_{\text{stat},b} \oplus \sigma_{\text{sys},b} \oplus \sigma_{\text{nlo},b}$$

$$\sigma^{\text{cor}}_b = \sigma_{\text{pol},b} \qquad \sigma^{\text{cor}}_b = \sigma_{\text{lum},b}$$

SMEFT asymmetry expressions:

$$A_{\text{SMEFT},b} = A_{\text{SM},b} + \sum_{k=1}^{N_{\text{fit}}} C_k \, \delta A_{k,b} + \mathcal{O}(C_k^2), \quad N_{\text{fit}} \in \text{Range}(7)$$

χ^2 function for each pseudoexperiment:

$$\chi^{2\,(e)} = \sum_{b,b'=1}^{N_{\text{bin}}} [A_{\text{SMEFT},b} - A^{(e)}_{\text{pseudo},b}] H_{bb'} [A_{\text{SMEFT},b'} - A^{(e)}_{\text{pseudo},b'}]$$

Polarimetry and luminosity difference can be limiting factors.

- ⇒ use data itself to constrain these systematic effects
- ⇒ simultaneous fits of C_k with beam polarization, P, and luminosity difference, A_{lum}, in an attempt to obtain stronger bounds for C_k

Fits of C_k with P:

$$\chi^{2\,(e)} = \sum_{b,b'=1}^{N_{\text{bin}}} \left[P A_{\text{SMEFT},b} - A^{(e)}_{\text{pseudo},b}\right] \left[H_{bb'}\Big|_{\sigma_{\text{pol}}\to 0} \right] \left[P A_{\text{SMEFT},b'} - A^{(e)}_{\text{pseudo},b'}\right] + \frac{(P-\bar{P})^2}{\delta P^2}$$

unpolarized PV asymmetries:

- $|\rho(C_k, P)| \gtrsim 0.7$
- 30-50% stronger bounds

polarized PV asymmetries:

- $|\rho(C_k, P)| \lesssim 0.2$
- 15-20% weaker bounds

Improvement is more significant than worsening ⇒ include P in fits.

Fits of C_k with A_{lum}:

$$\chi^{2\,(e)} = \sum_{b,b'=1}^{N_{\text{bin}}} \left[A_{\text{SMEFT},b} - A^{(e)}_{\text{pseudo},b} - A_{\text{lum}}\right] \left[H_{bb'}\Big|_{\sigma_{\text{lum}}\to 0} \right] \left[A_{\text{SMEFT},b'} - A^{(e)}_{\text{pseudo},b'} - A_{\text{lum}}\right]$$

Mild correlations, $|\rho(C_k, A_{\text{lum}})| \lesssim 0.4$, leading to 15-20% weaker bounds
⇒ do not include A_{lum} in fits.

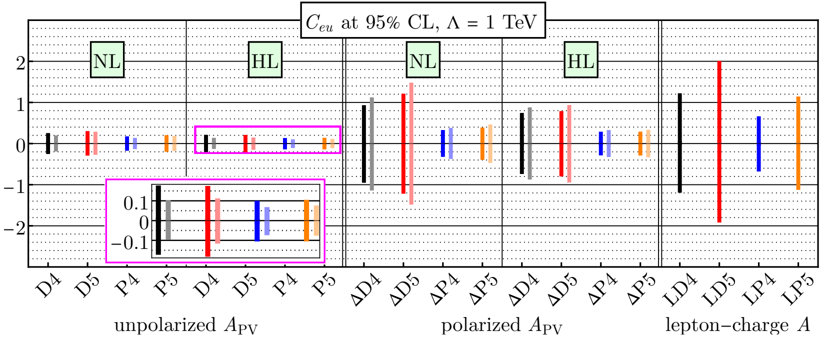

In terms of the strength of bounds:

- proton > deuteron
- low-lum. high-energy (4^{th} sets) > high-lum. low-energy (5^{th} sets)
- unpolarized PV > polarized PV > lepton-charge
- improvement: unpolarized PV > polarized PV if NL $\rightarrow$ HL

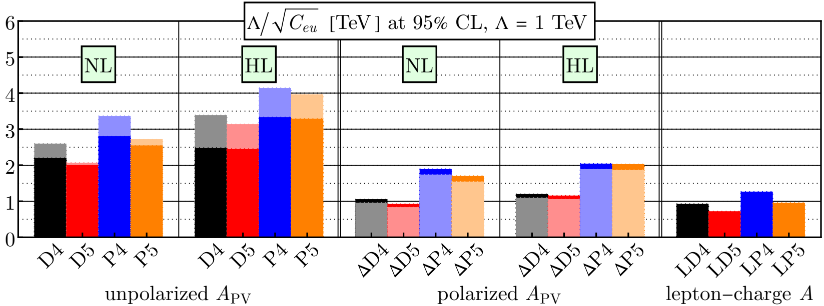

- UV scales ∼ 3 TeV in NL case
- UV scales ∼ 4 TeV in HL case

Compare the bounds from deuteron vs. proton data in the nominal-luminosity case for all the three types of asymmetries:

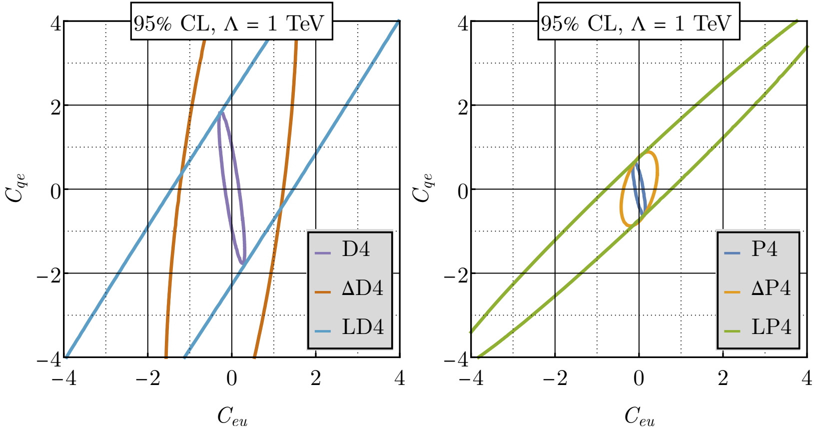

- Unpolarized PV asymmetries lead to strongest bounds.
- Proton data imposes stronger bounds.

Compare the bounds from deuteron and proton data of unpolarized PV asymmetries to the 8-TeV 20-fb^{-1} LHC NC DY data (Boughezal, Petriello, & Wiegand [2004.00748, 2104.03979]):

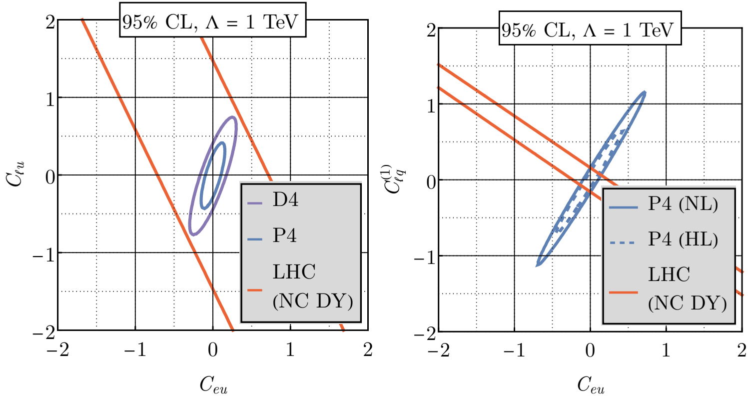

The LHC fits are highly degenerate and exhibit a flat direction, which remain even in the high-luminosity case. The EIC can resolve and constrain this parameter space strongly.

Compare proton data of unpolarized PV asymmetries to the 8-TeV 20-fb^{-1} LHC NC DY data (Boughezal, Petriello, & Wiegand [2004.00748]) when the LHC fit doesn't have a flat direction:

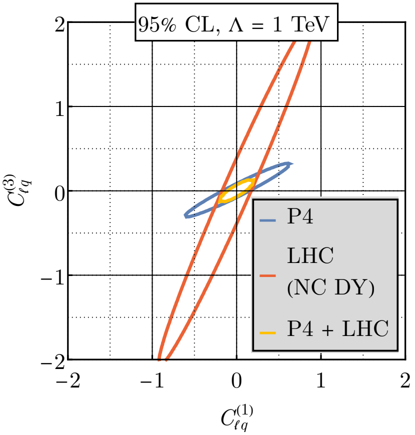

When the LHC fit gives a strong bound without showing a flat direction, the EIC can constrain the same parameter space even more strongly.

N_{fit}	N_{exp}
2	10^3
3	10^4
4	10^5
5	10^6
6	10^7
7	10^8(?!)

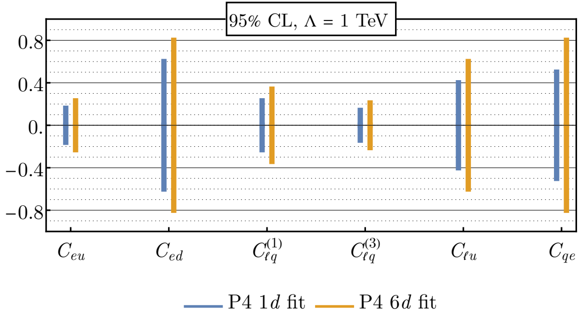

- Number of pseudoexperiments increases to reflect the required statistics.
- Beam polarization parameter, P, is not included here.
- Bounds become 25 to 40% weaker due to increased number of fitted parameters and correlations among them.

Compare the two-parameter fits of Wilson coefficients to the projections from a six-parameter fit:

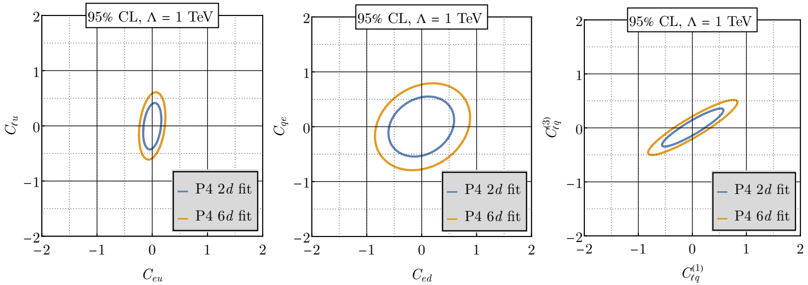

- The *eeuu* vertex contains the combination $C_{\ell q}^{(1)} - C_{\ell q}^{(3)}$ and the *eedd* vertex has $C_{\ell q}^{(1)} + C_{\ell q}^{(3)}$.
- These may lead to degeneracies and flat directions in a multi-parameter fits of Wilson coefficients.
- The EIC can resolve this part of the parameter space, imposing strong bounds.

- We investigate the BSM potential of EIC in the model-independent SMEFT framework by focusing on semi-leptonic four-fermion operators at dimension 6 by giving a detailed accounting of uncertainties.
- We obtain bounds on Wilson coefficients from single-, double-, and even multiple-parameter fits by using techniques to simultaneously fit P and A_{lum} together with SMEFT parameters.

- We find that UV scales up to 3 TeV (or 4 TeV) can be probed with nominal (or $10\times$ high) annual luminosity.
- We observe that the strongest bounds come from unpolarized PV asymmetries of proton.
- EIC is shown to be complementary and competitive to LHC NC DY by
  - equally or more strongly confining the Wilson coefficients with distinct correlations;
  - resolving the degeneracies observed in the LHC data.

EIC was designed as a QCD machine and it shows strong potential for BSM physics.